CI&CEQ

Available on line at
Association of the Chemical Engineers of Serbia AChE
www.ache.org.rs/CICEQ

Chemical Industry & Chemical Engineering Quarterly 19 (3) 321–331 (2013) CI&CEQ

HASSAN GOLMOHAMMADI[1]
ABBAS RASHIDI[2]
SEYED JABER SAFDARI[1]

[1]Nuclear Science and Technology Research Institute, AEOI, Tehran, Iran
[2]Department of Chemical Engineering, Faculty of Engineering, University of Mazandaran, Babolsar, Iran

SCIENTIFIC PAPER

UDC 66:004.8

DOI 10.2298/CICEQ120403066G

PREDICTION OF FERRIC IRON PRECIPITATION IN BIOLEACHING PROCESS USING PARTIAL LEAST SQUARES AND ARTIFICIAL NEURAL NETWORK

A quantitative structure-property relationship (QSPR) study based on partial least squares (PLS) and artificial neural network (ANN) was developed for the prediction of ferric iron precipitation in bioleaching process. The leaching temperature, initial pH, oxidation/reduction potential (ORP), ferrous concentration and particle size of ore were used as inputs to the network. The output of the model was ferric iron precipitation. The optimal condition of the neural network was obtained by adjusting various parameters by trial-and-error. After optimization and training of the network according to back-propagation algorithm, a 5-5-1 neural network was generated for prediction of ferric iron precipitation. The root mean square error for the neural network calculated ferric iron precipitation for training, prediction and validation set were 32.860, 40.739 and 35.890, respectively, which were smaller than those obtained by the PLS model (180.972, 165.047 and 149.950, respectively). The obtained results reveal the reliability and good predictivity of the neural network model for the prediction of ferric iron precipitation in bioleaching process.

Keywords: quantitative structure-property relationship; ferric iron precipitation; bioleaching process; partial least squares; artificial neural network.

Bioleaching employs the oxidation ability of bacteria to dissolve metal sulphides and help the extraction and recovery of valuable and base metals from main ores and concentrates [1,2]. Metal-winning processes derived from the activity of microorganisms propose a possibility to attain metal ions from mineral resources not available by traditional techniques. Microbes such as bacteria and fungi change metal compounds into their water-soluble types and are biocatalysts of this process called microbial leaching or bioleaching [3,4]. Recently, *Acidithiobacillus ferrooxidans* were believed to be the common significant microorganisms in the bioleaching of metal ions from ores [5].

Acidithiobacillus ferrooxidans is an acidophilic chemolithoautotrophic proteobacterium that achieves its energy from the oxidation of ferrous iron, elemental sulfur, or partially oxidized sulfur compounds [6]. Owing to its capacity of oxidation, *Acidithiobacillus ferrooxidans* has abundant industrial appliances in biohydrometallurgy. The most important applications can be established in the field of mining [7] where the oxidative effects are utilized for the bioleaching of different metals such as copper from minerals like pyrite or chalcopyrite [8,9] or even uranium [10].

The mechanism of uranium extraction assisted by the indirect oxidation purpose of this microbe is probably as follows:

$$UO_2 + Fe_2(SO_4)_3 \rightarrow UO_2SO_4 + 2FeSO_4 \quad (1)$$

$$U^{4+} + 2Fe^{3+} \rightarrow U^{6+} + 2Fe^{2+} \quad (2)$$

Uranium is barely soluble in an aqueous environment when it is in the +4 oxidation state; however, in an acidic medium the ferric iron oxidizes U^{4+} to U^{6+}, which is easily dissolved. As a conjugate reaction to the oxidation of U^{4+}, the ferric iron reduces to ferrous iron and through the oxidation function of *Acidithiobacillus ferrooxidans* it is re-oxidized back to the ferric state which is then able to continue oxidizing U^{4+} to U^{6+}.

Correspondence: H. Golmohammadi, Nuclear Science and Technology Research Institute, AEOI, P.O. Box 11365-3486, Tehran, Iran.
E-mail: Hassan.gol@gmail.com
Paper received: 3 April, 2012
Paper revised: 20 June, 2012
Paper accepted: 20 June, 2012

Temperature and pH of leaching solution can vary widely in the completeness of time. In addition, as the values of this parameter increase, ferric iron precipitation increases and consequently the leaching efficiency reduce. Therefore, it is very important to predict ferric iron concentration recycled by a comprehensive model for the design, monitoring and organization of bioleaching operations.

As an alternative to physical models, artificial neural networks (ANNs) are a valuable estimate tool. Up to now, numerous applications of ANN models in the engineering area were reported. For example, Laberge *et al*. applied ANN to predict the metal (Cu, Zn and Cd) solubilization percentages in municipal sludge treated with a continuous bioleaching process [11]. Jorjani *et al.* used ANN to estimate the effects of operational parameters on the organic and inorganic sulfur removal from coal by sodium butoxide [12]. Acharya and co-workers developed a neural network to model the extent of sulphur removal from three types of coal using native cultures of Acidithiobacillus ferrooxidans [13]. Diamond *et al*. utilized ANN for the Study of pH on the fungal treatment of red mud [14]. Nikhil *et al*. employed ANN for prediction of H_2 production rates in a sucrose-based bioreactor system [15]. They also modeled the performance of a biological Fe^{2+} oxidizing fluidized bed reactor (FBR) by a popular neural network-back-propagation algorithm under different operational conditions [16]. Yetilmezsoy and Demirel used a three-layer artificial neural network (ANN) model to predict the efficiency of Pb(II) ions removal from aqueous solution by Antep pistachio (*Pistacia vera* L.) shells based on 66 experimental sets obtained in a laboratory batch study [17]. Daneshvar *et al*. employed an artificial neural network (ANN) to model decolorization of textile dye solution containing C.I. Basic Yellow 28 by electrocoagulation process [18]. Sahinkaya and co-workers developed an artificial neural network model for estimation of the performance of a fluidized-bed reactor (FBR) based sulfate reducing bioprocess and control the operational conditions for improved process performance [19]. Sahinkaya also modeled the biotreatment of zinc-containing wastewater in a sulfidogenic CSTR by using artificial neural network [20].

Thus, to successfully extract the costly metals from the minerals, the suitable process and control of bioleaching purposes have become very essential. In relation to recent considerations, the dissolution of metals happens only chemically with the assist of ferric ions, which operate as oxidizing agents. Superior control of bioleaching may be acquired by using a strong model to predict convinced key factors derived from past surveillances [21]. Models rooted in ANNs may be efficiently employed in bioleaching applications and very helpful at arresting the nonlinear correlations existing between variables in complex systems like bioleaching. The main aim of this investigation is using this aptitude of artificial neural network for prediction of ferric iron precipitation in bioleaching process. In this study, an artificial neural network method using the back-propagation algorithm was proposed for the prediction of ferric iron precipitation in uranium bioleaching process under different operational conditions.

MATERIAL AND METHODS

Uranium ores

The uranium ores used in the experiments was supplied by the Nuclear Science and Technology Research Institute, AEOI. The ore was ground using mortar and then sieved. The particle size of the sieved material ranged from 70 to 500 μm, with an average particle size of 100±10 μm.

Microorganism and culture

The medium for *Acidithiobacillus ferrooxidans* growth was 9K medium which is a mixture of mineral salts ($(NH_4)_2SO_4$, 3.0 g/l, K_2HPO_4, 0.5 g/l, $MgSO_4{\cdot}7H_2O$, 0.5 g/l, KCl, 0.1 g/l and $Ca(NO_3)_2$, 0.01g/l). $FeSO_4{\cdot}7H_2O$ was added as energy source. The pH of the medium was adjusted to 2.0 using 2.0 M H_2SO_4. The culture was cultivated at 35 °C for 2-3 days before centrifugation. The yield cells of *Acidithiobacillus ferrooxidans* were suspended in a fresh solution of the mineral salt medium for the preparation of the bacterial concentrate [22].

Bioleaching experiments

The experiments were performed in 250 ml Erlenmeyer flasks containing 5 g of ore and 100 ml of 9K medium. Erlenmeyer flasks covered with hydrophobic cotton to admit oxygen but reduce water loss through evaporation. Control experiments were carried out without bacteria and with 2% bactericide agent (formaldehyde). The concentrations of Fe were 2 and 4 g/l using $FeSO_4{\cdot}7H_2O$. Each experiment was accomplished twice under same standard conditions at 30-40 °C, 180 rpm shaking speed and pH 2.0 [23]. A known amount of sample was drawn at 6 days interval for analysis of Iron. The pH of the leach solution was maintained daily with 2 M sulfuric acid. The oxidation/reduction potential (ORP) was measured against saturated calomel electrode (SCE).

Analytical procedures

Total iron was analyzed using the PG T80+ UV/Vis spectrometer according to Karamanev method [24]. The ferrous iron concentration was determined using PG T80+ UV/Vis spectrometer by the modified colorimetric orthophenantroline method [25]. A Metrohm pH meter (model 827) with a combined glass electrode was used for pH measurements. The changes in oxidation/reduction potential (ORP) were monitored using an ORP meter (Metrohm model 827).

Partial least squares model for the prediction of ferric iron precipitation

PLS is a familiar multivariate method [26-28], which provides a stepwise solution for a regression model. It extracts principal component-like latent variables from original independent variables (predictor variables) and dependent variables (response variables), respectively. Assume that **X** characterizes independent variables (**X** is a matrix) and Y represents dependent variables (Y is a vector). Then a brief description of computations is given as follows:

$$\mathbf{X} = \mathbf{T}\mathbf{P}^{\mathbf{T}} + \mathbf{E} \quad (3)$$

$$Y = QS^{\mathbf{T}} + \mathbf{F} \quad (4)$$

The matrices **E** and **F** include residual for **X** and Y, respectively. **T** and **P** are score and loading matrices associated with the **X**, Q and S are the score and loading of Y and superscript **T** indicates the transposed matrix. The relationship between scores and dependent variable is obtained from:

$$Y = \mathbf{T}\mathbf{B}Q^{\mathbf{T}} + \mathbf{F} \quad (5)$$

where **B** is the matrix of the regression coefficient achieved by a least squares procedure. The PLS algorithm used in this study was the singular value decomposition (SVD)-based PLS. This algorithm was proposed by Lobert *et al.* in 1987 [29]. A concise discussion of the SVD-based PLS algorithm can be found in the literature [30-32]. The program of PLS modeling based on SVD was written with MATLAB 7 in our laboratory [33].

Artificial neural network model for the prediction of ferric iron precipitation

An artificial neural network is a kind of artificial intelligence that emulates some purpose of the human brain. Neural networks are general-purpose computing techniques that can solve complex nonlinear problems. The network comprises abundance of simple processing elements linked to each other by weighted connections along with a specified architecture. These networks learn from the training data by altering the connection weights [34]. A detailed explanation of the theory behind a neural network has been sufficiently described elsewhere [35-37]. Therefore, only the points related to this work are illustrated here. An essential procession element of an ANN is a node. Each node has a series of weighted inputs, W_{ij}, and performs as a summing point of weighted input signals. The summed signals pass through a transfer function that may be in sigmoidal form. The output of node j, O_j, is given by Eq.(6):

$$O_j = 1/(1 + \exp(-\mathbf{X})) \quad (6)$$

where X is defined by the following equation:

$$\mathbf{X} = W_{ij}O_i + B_j \quad (7)$$

In Eq. (7), B_j is a bias term, O_i is the output of the node of the previous layer and W_{ji} represents the weight between the nodes of i and j.

A feed-forward neural network consists of three layers. The first layer (input layer) consists of nodes and operates as an input buffer for the data. Signals introduced to the network, with one node per element in the sample data vector, pass through the input layer to the layer called the hidden layer. Each node in this layer sums the inputs and forwards them through a transfer function to the output layer. These signals are weighted and then pass to the output layer. In the output layer the processes of summing and transferring are repeated. The output of this layer now signifies the calculated value for the node k of the network.

As well as the network topology, a significant constituent of nearly all neural networks is a learning rule. A learning rule permits the network to alter its connection weights so as to correlate given inputs with corresponding outputs. The training of the network has been performed by using a back-propagation algorithm, in which the network reads inputs and outputs from an appropriate data set (training set) and iteratively calculates weights and biases to facilitate decrease the sum of squared dissimilarities between predicted and target values. The training is stopped when the error in prediction achieves a preferred level of accuracy. However, if the network is gone to train too long, it will overtrain and misplace the aptitude to prediction. In order to avoid overtraining, the predictive recital of the trained ANN is controlled by running the back-propagation algorithm on a data set not used in training.

Neural networks are rooted in the principle that an extremely unified system of effortless processing elements can learn intricate interrelationships between independent and dependent variables. The perfor-

mance and properties of such a network is reliant on the computational elements, especially the weights and the transfer function, in addition to the net topology. Usually the network topology and the transfer function are particular in advance and are kept fixed, so just the weights of the synaptic connections and the number of neurons in the hidden layer need to be evaluated. The error function should be minimized so that the neural network accomplishes the finest performance. Dissimilar algorithms have been grown to minimize the error function. The most traditional is the so-called back-propagation (BP) algorithm, which belongs to the group of supervised learning methods. The error at the output layer in a BP neural network propagates rearward to the input layer during the hidden layer in the network to acquire the final beloved output. The gradient descent technique is employed to compute the weights of the network and regulate the weights of interconnections to minimize the output error. In this work, multi layered feed forward neural networks were used, which utilized the algorithm of back-propagation of errors and a gradient-descent technique, known as the "delta rule" [38,39] for the adjustment of the connection weights (further called BP networks). BP networks include one input layer, one (or possibly several) hidden layer(s) and an output layer. The number of nodes in the input and output layers are described by the difficulty of the problem being solved. The input layer collects the experimental information and the output layer encloses the response sought. The hidden layer codes the information attained from the input layer, and transports it to the output layer. The number of nodes in the hidden layer may be considered as an adjustable factor.

In the present work, an ANN program was written with MATLAB 7. This network was feed-forward fully connected and had three layers with tangent sigmoid transfer function (tansig) at the hidden layer and linear transfer function (purelin) at the output layer. The operational conditions of the bioleaching process were used as inputs of the network and its output signal represents the ferric iron precipitation. Therefore, this network has five nodes in input layer and one node in output layer. The value of each input was divided into its mean value to bring them into the dynamic range of the sigmoidal transfer function of the network. The initial values of weights were randomly selected from a uniform allocation that ranged between -0.3 to +0.3 and the initial values of biases were set to be 1. These values were optimized during the network training. The back-propagation algorithm was used for the training of the network. Before training, the network parameters would be optimized. These parameters are: number of nodes in the hidden layer, weights and biases learning rates and the momentum. Procedures for the optimization of these descriptors were reported elsewhere [38,39]. Then the optimized network was trained using a training set for adjustment of weights and biases values. To maintain the predictive authority of the network at an enviable level, training was stopped when the value of error for the prediction set started to increase. Since the prediction error is not a good evaluation of the generalization error, the prediction potential of the model was assessed on a third set of data, named validation set. Experiments in the validation set were not used during the training process and were reserved to evaluate the predictive power of the generated ANN.

Evaluation of the predictive ability of a QSPR model

For the optimized QSPR model, numerous parameters were chosen to test the prediction capability of the model. A real QSPR model may have a high predictive aptitude, if it is close to ideal one. This may involve that the correlation coefficient R between the experimental (actual) y and predicted $\tilde{y}$ properties must be close to 1 and regression of y against $\tilde{y}$ or $\tilde{y}$ against y through the origin, *i.e.*, $y^{r0} = k\tilde{y}$ and $\tilde{y}^{r0} = k'y$, respectively, should be illustrated by at least either k or k' close to 1 [40]. Slopes k and k' are calculated as follows:

$$k = \frac{y_i \tilde{y}_i}{\tilde{y}_i^2} \tag{8}$$

$$k' = \frac{y_i \tilde{y}_i}{y_i^2} \tag{9}$$

The criteria formulated above may not be adequate for a QSPR model to be really predictive. Regression lines through the origin defined by $y^{r0} = k\tilde{y}$ and $\tilde{y}^{r0} = k'y$ (with the intercept set to one) should be close to optimum regression lines $y^r = a\tilde{y} + b$ and $\tilde{y}^r = a'y + b'$ (b and b' are intercepts). Correlation coefficients for these lines R_0^2 and R'^2_0 are calculated as follows:

$$R_0^2 = 1 - \frac{(\tilde{y}_i - y_i^{r0})^2}{(\tilde{y}_i - \bar{\tilde{y}})^2} \tag{10}$$

$$R'^2_0 = 1 - \frac{(y_i - \tilde{y}_i^{r0})^2}{(y_i - \bar{y})^2} \tag{11}$$

where $\bar{y}$ and $\bar{\tilde{y}}$ are the average values of the observed and predicted properties, respectively, and the summations are over all n compounds in the validation set.

A difference between R_2 and R_0^2 values (R_m^2) desires to be studied to examine the prediction potential of a model [41]. This term was defined in the following manner:

$$R_m^2 = R^2\left(1-\left|\sqrt{R^2-R_0^2}\right|\right) \quad (12)$$

Finally, the following criteria for evaluation of the predictive ability of QSPR models should be considered:

1. High value of cross-validated R^2 ($q^2 > 0.5$).
2. Correlation coefficient R between the predicted and actual properties from an external test set close to 1. R_0^2 or R'^2_0 should be close to R^2.
3. At least one slope of regression lines (k or k') through the origin should be close to 1.
4. R_m^2 should be greater than 0.5.

Diversity validation

The essential investigated theme in chemical database analysis is the diversity of sampling [42]. The diversity problem involves defining a different division of representative compounds. In this study, diversity analysis was done on the data set to make sure that the structures of the training, prediction or validation sets can characterize those of the whole ones. We consider a database of n experiments generated from m highly correlated variable $\{\mathbf{X}_J\}_{j=1}^{m}$. Each experiment, $\mathbf{X}_i$, is represented as following vector:

$$\mathbf{X}_i = (x_{i1}, x_{i2}, x_{i3}, \ldots x_{im}) \text{ for } i = 1,2,\ldots,n \quad (13)$$

where x_{ij} indicates the value of variable j of experiment $\mathbf{X}_i$. The collective database $\mathbf{X} = \{\mathbf{X}_i\}_{i=1}^{N}$ is represented a $n \times m$ matrix of $\mathbf{X}$ as follows:

$$\mathbf{X} = (X_1, X_2, \ldots, X_N)^{\mathbf{T}} = \begin{bmatrix} x_{11} & x_{12} & \ldots & x_{1m} \\ x_{21} & x_{22} & \ldots & x_{2m} \\ \vdots & \vdots & \ddots & \vdots \\ x_{n1} & x_{n2} & \ldots & x_{nm} \end{bmatrix} \quad (14)$$

where the superscript $\mathbf{T}$ represents the vector/matrix transpose. A distance score, d_{ij}, for two different experiments, $\mathbf{X}_i$ and $\mathbf{X}_j$, can be measured by the Euclidean distance norm:

$$d_{ij} = \|\mathbf{X}_i - \mathbf{X}_j\| = \sqrt{\sum_{k=1}^{m}(x_{ik} - x_{jk})^2} \quad (15)$$

The mean distances of one experiment to the remaining ones were computed as:

$$\bar{d}_i = \frac{\sum_{j=1}^{n} d_{ij}}{n-1}, \; i = 1,2,\ldots,n \quad (16)$$

Then the mean distances were normalized within the interval of zero to one. In order to calculate the values of mean distances in accordance with Eqs. (15) and (16), a MATLAB program was written that combines maximum dissimilarity search algorithms and general multi-dimensional measurements of chemical similarity rooted in different experiments. The closer to one the distance is, the more diverse to each other the compound is. The mean distance of experiments were plotted against ferrous iron precipitation (EXP) (Figure 1), which shows the diversity of the experiments in the training, prediction and validation sets. As can be seen from this figure, the experiments are diverse in all sets and the training set with a broad representation of the chemistry space was adequate to ensure the model's stability and the diversity of prediction and validation sets can prove the predictive capability of the model.

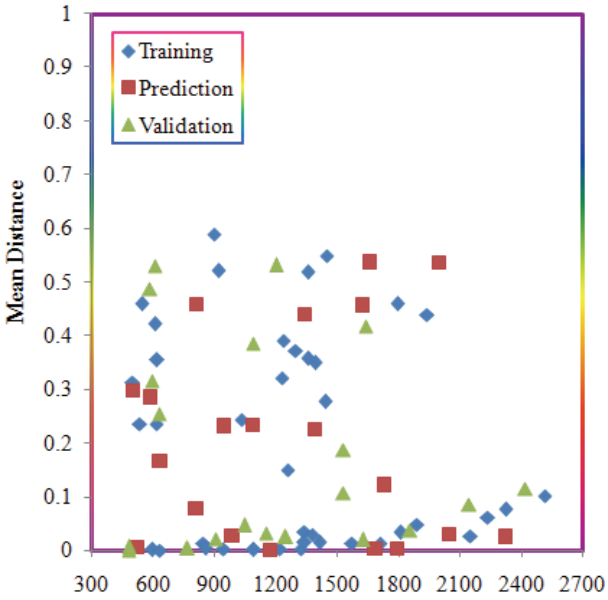

Figure 1. Scatter plot of experiments for training, prediction and validation sets.

RESULTS AND DISCUSSION

PLS Modeling

The descriptive statistics of corresponding observed PLS and ANN predicted values of ferric iron precipitation of all experiments studied in this work are shown in Table 1. The independent variables of leaching temperature, initial pH, oxidation/reduction potential (ORP), ferrous iron concentration and particle size of uranium ore were used in the develop-

Table 1. Descriptive statistics of observed and predicted values of ferric iron precipitation (mg/l); EXP refers to experimental; PLS refers to partial least squares; ANN refers to artificial neural network

Set	n	Minimum	Maximum	Mean	Standard deviation
Training (EXP)	40	317	2514	1282	572
Training (PLS)	40	304	2489	1308	556
Training (ANN)	40	314	2498	1279	568
Prediction (EXP)	20	506	2327	1298	586
Prediction (PLS)	20	381	2271	1306	565
Prediction (ANN)	20	512	2310	1296	582
Validation (EXP)	20	486	2421	1207	607
Validation (PLS)	20	392	2377	1213	558
Validation (ANN)	20	492	2415	1206	600

ment of PLS method. By interpreting the variables in the models, it is possible to gain some insight into factors that are probable related to ferric iron precipitation. For assessment of the relative importance and donation of each variable in the model, the value of mean effect (ME) was calculated for each variable by the following equation:

$$ME_j = \frac{\beta_j \sum_{i=1}^{n} d_{ij}}{\sum_{j}^{m} \beta_j \sum_{i=1}^{n} d_{ij}} \quad (17)$$

where ME_j is the mean effect for considered variable j, β_j is the coefficient of variable j, d_{ij} is the value of interested variables for each experiment, and m is the number of variables in the model. The calculated values of MEs are represented in the last column of Table 2 and are also plotted in Figure 2. Table 3 represents the correlation matrix for these variables. The value and sign of mean effect demonstrates the relative contribution and direction of influence of each variable on the ferric iron precipitation. As shown in Table 2, the most relevant variables based on their mean effects are pH and leaching temperature. The positive coefficient of these variables mean as the value of this variables increase, the values of ferric iron precipitation increase. These results are in accordance with those we have obtained in bioleaching experiments.

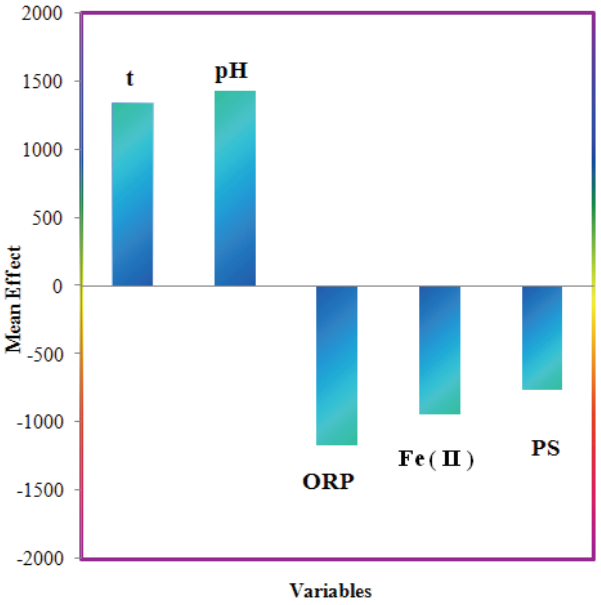

Figure 2. Plot of descriptor's mean effects.

Neural network modeling

The next step was the production of ANN and training of it. Input and output data normalization is a significant feature of training the network and performed to avoid problems with saturation of the neuron transfer function. Input and output data are typically normalized in the range (0,1) or (-1,+1). The type of normalization is problem dependent and may have

Table 2. The partial least squares regression coefficients

Variable	Notation	Coefficient	Mean effect
Leaching temperature	t	38.75	1345.67
Initial pH	pH	732.43	1432.27
Oxidation/reduction potential	ORP	-2.28	-1173.20
Ferrous iron concentration	Fe (II)	-1.16	945.13
Particle size	PS	-8.50	-765.00
Constant	-	13666.56	-

Table 3. Correlation matrix between selected variables

	t	pH	ORP	Fe (II)	PS
t	1	-0.029	0.213	-0.124	0.144
pH		1	-0.668	0.750	0.196
ORP			1	-0.642	0.251
Fe (II)				1	-0.097
PS					1

some effects on how well the ANN trains. Here we use Scaled normalization to bring the data into dynamic range of the tangent sigmoid transfer function of the network. Before training the ANNs, the parameters of network including the number of nodes in the hidden layer, weights and biases learning rates and momentum values were optimized. In order to determine the optimum number of nodes in hidden layer several training sessions were conducted with different number of hidden nodes. The values of standard error of training (SET) and standard error of prediction (SEP) were calculated after each 1000 iterations and calculation was stopped when overtraining began, then SET and SEP values were recorded. The recorded values of SET and SEP were plotted against the number of nodes in hidden layer, and the number of hidden nodes with minimum values of SET and SEP was chosen as the optimum one (Figure 3). It can be seen from this figure that 6 nodes in the hidden layer were sufficient for a good performance of the network. Learning rates of weights and biases and also momentum values were optimized in a similar way and the results are shown in Figures 4-6, respectively. As can be seen, the optimum values of the weights and biases learning rates and momentum were 0.2, 0.2 and 0.3, respectively. The generated ANN was then trained by using the training set for the optimization of weights and biases. However, training was stopped when overtraining began. For the evaluation of the prediction power of network, trained ANN was used to simulate the ferric iron precipitation included in the prediction set.

Table 4 shows the architecture and specification of the optimized network. After optimization of the network parameters, the network was trained by using training set for adjustment of the weights and biases values by back-propagation algorithm. It is recognized that the neural network can become overtrained. An overtrained network has usually learned completely the motivation pattern it has seen but cannot give precise forecasting for unobserved stimuli, and it would no longer be capable to generalize. There are various methods for overcoming this problem. One method is to utilize a prediction set to assess the prediction power of the network during its training. In this method, after each 1000 training iterations, the

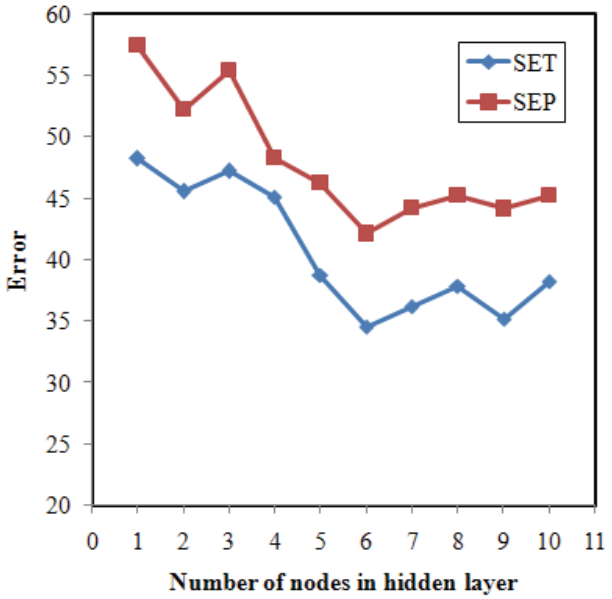

Figure 3. The values of SET and SEP versus number of nodes in hidden layer.

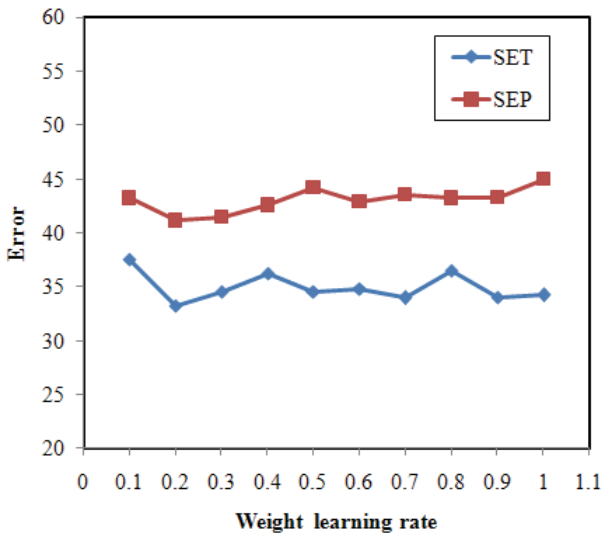

Figure 4. The values of SET and SEP versus weight learning rate.

network was used to calculate ferric iron precipitation included in the prediction set. To preserve the predictive power of the network at an enviable level, training was stopped when the value of errors for the prediction set started to increase.

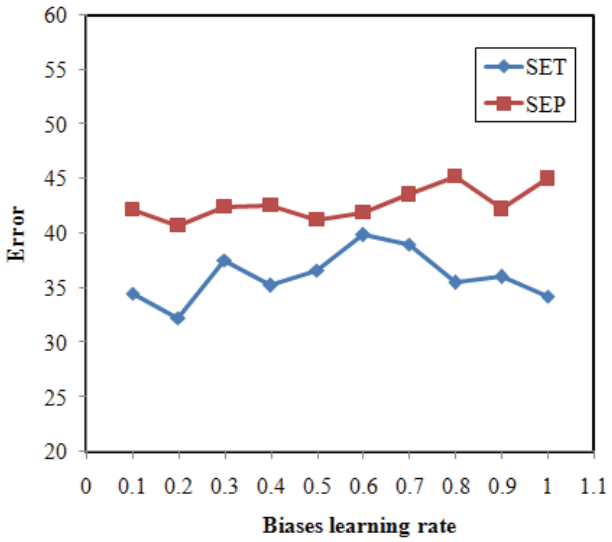

Figure 5. The values of SET and SEP versus biases learning rate.

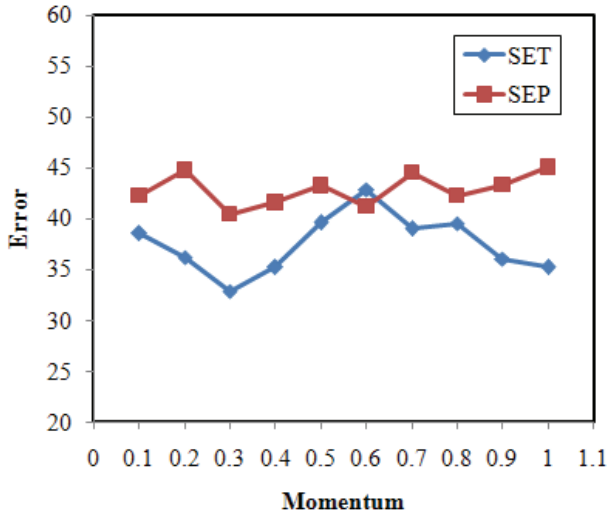

Figure 6. The values of SET and SEP versus momentum.

The predictive power of the ANN models developed on the selected training sets are estimated on the predictions of validation set chemicals, by calculating the q^2 that is defined as follow:

$$q^2 = 1 - \frac{\sum(y_i - \hat{y}_i)^2}{\sum(y_i - \bar{y})^2} \quad (18)$$

where y_i and $\hat{y}_i$, respectively are the measured and predicted values of the dependent variable (ferric iron precipitation), $\bar{y}$ is the averaged value of dependent variable of the training set and the summations cover all the compounds. The calculated value of q^2 was 0.996.

Table 4. Architecture and specifications of optimized ANN model

Parameter	Value
Number of nodes in the input layer	5
Number of nodes in the hidden layer	6
Number of nodes in the output layer	1
Weights learning rate	0.2
Biases learning rate	0.2
Momentum	0.3
Transfer function (hidden layer)	Tangent sigmoid
Transfer function (output layer)	Linear

Table 1 shows the descriptive statistics of observed and predicted values of ferric iron precipitation for the training, prediction and validation sets. The statistical parameters obtained by ANN and PLS models for these sets are shown in Table 5. The standard errors of training, prediction and validation sets for the PLS model are 180.972, 165.047 and 149.950, respectively, which would be compared with the values of 32.860, 40.739 and 35.890, respectively, for the ANN model. Comparison between these values and other statistical parameters in Table 5 discloses the superiority of the ANN model over PLS ones. The key power of neural networks, unlike regression analysis, is their aptitude to supple mapping of the selected features by manipulating their functional dependence implicitly.

The statistical values of validation set for the ANN model was characterized by q^2 = 0.996, R^2 = = 0.996 (R = 0.998), $R_0^2 = 0.996$, $R_m^2 = 0.988$ and k = = 1.002. These values and other statistical parameters (Table 5) reveal the high predictive ability of the model. Figure 7 shows the plot of the ANN predicted versus experimental values for ferric iron precipitation of all of the experiments in data set. The residuals of the ANN calculated values of the ferric iron precipi-

Table 5. Statistical parameters obtained using the ANN and PLS models; R is the correlation coefficient, SE is standard error and F is the statistical F value

Model	SET	SEP	SEV	R_T	R_P	R_V	F_T	F_P	F_V
ANN	32.860	40.739	35.890	0.998	0.997	0.998	10400	3517	4727
PLS	180.972	165.047	149.950	0.943	0.957	0.966	306	197	254

tation are plotted against the experimental values in Figure 8. The propagation of the residuals on both sides of the zero line signifies that no systematic error exists in the constructed QSPR model.

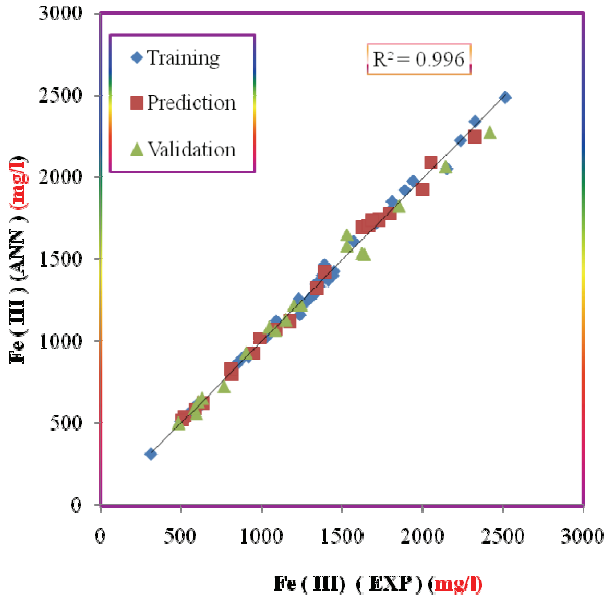

Figure 7. Plot of calculated ferric iron precipitation against experimental values.

CONCLUSIONS

Results of this study disclose that ANN can be used successfully in development of a QSPR model to predict the ferric iron precipitation in uranium bioleaching process. Variables appearing in this QSPR model such as leaching temperature, initial pH, oxidation/reduction potential, ferrous concentration and particle size of uranium ore provide some information related to different experiments which can affect the ferric iron precipitation. The good agreement between experimental results and predicted values verifies the validity of obtained models. The calculated statistical parameters of these models reveal the superiority of ANN over PLS model. The results show that the ANN model can accurately describe the relationship between the operational conditions of bioleaching process and ferric iron precipitation.

Nomenclature

QSPR	Quantitative structure-property relationship
ANN	Artificial neural network
PLS	Partial least squares
ORP	Oxidation/reduction potential
PS	Particle size
R	Correlation coefficient
ME	Mean effect
t	Leaching temperature
SE	Standard error
F	Statistical *F* value
FBR	Fluidized bed reactor
W	Weight signal
O	Output of the node
B	Bias term
k	Slope of regression line
EXP	Experimental
q	Cross validated coefficient
SCE	Saturated calomel electrode
X	Predictor (independent) variable
Y	Response (dependent)variable
T	Score of **X**

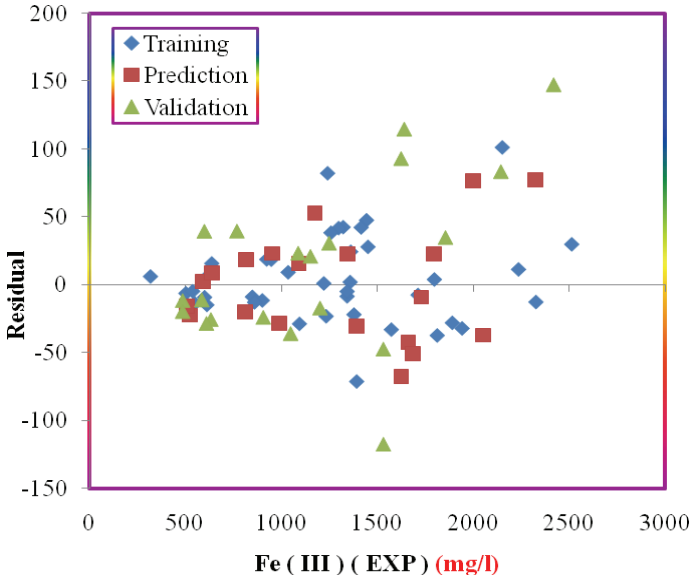

Figure 8. Plot of residual versus experimental values of ferric iron precipitation.

P Loading of **X**
Q Score of Y
S Loading of Y
E Residual for **X**
F Residual for Y
BP Back-propagation
d Distance score
SET Standard error of training
SEP Standard error of prediction
SEV Standard error of validation

REFERENCES

[1] K. Bosecker, FEMS Microbiol. Rev. **20** (1997) 591-604

[2] D. Holmes, Chem. Ind. **1** (1999) 20-24

[3] S. Ilyas, M.A. Anwar, S.B. Niazi, M.A. Ghauri, B. Ahmad, K.M. Khan, J. Chem. Soc. Pak. **30** (2008) 61-68

[4] G.J. Olson, J.A. Brierley, C.L. Brierley, Appl. Microbiol. Biotechnol. **63** (2003) 249-257

[5] D.P. Kelly, A.P. Wood, Int. J. Syst. Evol. Microbiol. **50** (2000) 511-516

[6] D.E. Rawlings, Annu. Rev. Microbiol. **56** (2002) 65-91

[7] [7] J.A. Brierley, C.L. Brierley, Hydrometallurgy **59** (2001) 233-239

[8] T. Sugio, M. Wakabayashi, T. Kanao, F. Takeuchi, Biosci. Biotechnol. Biochem. **72** (2008) 998-1004

[9] S.M. Mousavi, S. Yaghmaei, M. Vossoughi, A. Jafari, S.A. Hoseini, Hydrometallurgy **80** (2005) 139-144

[10] J.A. Munoz, F. Gonzalez, A. Ballester, M.L. Blazquez, FEMS Microbiol. Rev. **11** (1993) 109-119

[11] C. Laberge, D. Cluis, G. Mercier, Water Res. **34** (2000) 1145-1156

[12] E. Jorjani, S. Chehreh Chelgani, S.H. Mesroghli, Fuel **87** (2008) 2727-2734

[13] C. Acharya, S. Mohanty, L.B. Sukla, V.N. Misra, Ecol. Model. **190** (2006) 223-230

[14] D. Diamond, D.S. Jyotsna, Res. J. Chem. Sci. **1** (2011) 108-112

[15] Nikhil, B. Özkaya, A. Visa, C.Y. Lin, J.A. Puhakka, O. Yli-Harja, World Academy of Science, Engineering and Technology **37** (2008) 20-25

[16] N.B. Ozkaya, E. Sahinkaya, P. Nurmi, A.H. Kaksonen, J.A. Puhakka, Bioprocess. Biosyst. Eng. **31** (2008) 111--117

[17] K. Yetilmezsoy, S. Demirel, J. Hazard. Mater. **153** (2008) 1288-1300

[18] N. Daneshvar, A.R. Khataee, N. Djafarzadeh, J. Hazard. Mater. **137** (2006) 1788-1795

[19] E. Sahinkaya, B. Ozkaya, A.H. Kaksonen, J.A. Puhakka, Biotechnol. Bioeng. **97** (2006) 780-787

[20] E. Sahinkaya, J. Hazard. Mater. **164** (2009) 105-113

[21] K. Yetilmezsoy, B. Ozkaya, M. Cakmakci, Neural Network World **31** (2011) 193-218

[22] K.D. Mehta, B.D. Pandey, T.R. Mankhand, Miner. Eng. **16** (2003) 523-527

[23] M.S. Choi, K.S. Cho, D.S. Kim, H.W. Ryu, J. Microbiol. Biotechnol. **21** (2005) 377-380

[24] D.G. Karamanev, L.N. Nilolov, V. Mamatarkova, Miner. Eng. **15** (2002) 341-346

[25] L. Herrera, P.R. Ruiz, J.C. Aguillon, A. Fehrmann, J. Chem. Tech. Biotechnol. **44** (1989) 171-181

[26] P. Geladi, B.R. Kowalski, Anal. Chim. Acta **185** (1986) 1-17

[27] B.S. Dayal, J.F. MacGregor, J. Chemom. **11** (1997) 73-85

[28] S. Ranar, P. Geladi, F. Lindgren, S.Wold, J. Chemom. **9** (1995) 459-470

[29] A. Lorber, L. Wangen, B.R. Kowalsky, J. Chemom. **11** (1987) 9-31

[30] T. Khayamian, A.A. Ensafi, B. Hemmateenejad, Talanta **49** (1999) 587-596

[31] M. Shamsipur, B. Hemmateenejad, M. Akhond, H. Sharghi, Talanta **54** (2001) 1113-1120

[32] A. Hoskuldsson, Chemom. Intell. Lab. Syst. **55** (2001) 23--38

[33] MATLAB 7.0, The Mathworks Inc., Natick, MA, USA, http://www.mathworks.com

[34] C.M. Bishop, Neural networks for pattern recognition Clarendon Press, Oxford, 1995

[35] J. Zupan, J. Gasteiger, Neural Network in Chemistry and Drug Design, Wiley-VCH, Weinheim, 1999

[36] T.M. Beal, H.B. Hagan, M. Demuth, Neural Network Design, PWS, Boston, MA, 1996

[37] J. Zupan, J. Gasteiger, Neural Networks for Chemists: An Introduction, VCH, Weinheim, 1993

[38] T.B. Blank, S.T. Brown, Anal. Chem. **65** (1993) 3081-3089

[39] M. Jalali-Heravi, M.H. Fatemi, J. Chromatogr., A **915** (2001)177-183

[40] A. Golbraikh, A. Tropsha, J. Mol. Graphics. Modell. **20** (2002) 269-276

[41] P.P. Roy, K. Roy, QSAR Comb. Sci. **27** (2008) 302-313

[42] A.G. Maldonado, J.P. Doucet, M. Petitjean, Mol. Divers. **10** (2006) 39-79.

HASSAN GOLMOHAMMADI
ABBAS RASHIDI
SEYED JABER SAFDARI

Nuclear Science and Technology Research Institute, AEOI, Tehran, Iran

NAUČNI RAD

PREDVIĐANJE PRECIPITACIJE FERI JONA U PROCESU BIOLUŽENJA PRIMENOM PARCIJALNIH NAJMANJIH KVADRATA I VEŠTAČKE NEURONSKE MREŽE

Razvijena je kvanitativna zavisnost između strukture i svojstava zasnovana na parcijalnim najmanjim kvadratima i veštačkoj neuronskoj mreži u cilju predviđanja precipitacije gvožđe(III) jona u procesu bioluženja. Ulazne promenljive bile su: temperatura luženja, početni pH, oksido-redukcioni potencijal, koncentracija gvožđe(II) i veličina čestica rude. Izlaz iz modela je bila precipitacija gvožđe(III) jona. Optimalni uslov veštačke neuronske mreže je dobijen podešavanjem različitih parametara metodom probe i greške. Posle optimizovanja i učenja mreže pomoću algoritma sa povratnom propagacijom, generisana je neuronska mreža 5-5-1 radi predviđanja precipitacije gvožđe(III) jona. Vrednosti korena srednje kvadratne greške za učenje, predviđanje i validaciju neuronske mreže bile su 32,860; 40,739 i 35,890, redom, koje su manje od onih dobijenih modelom parcijalnih najmanjih kvadrata (180,972; 165,047 i 149,950, redom). Dobijeni rezultati pokazuju pouzdanost i dobru prediktivnost neuronske mreže za predviđanja precipitacije gvožđe(III) jona u procesu bioluženja.

Ključne reči: kvanitativna zavisnost struktura-svojstvo, precipitacija gvožđe(III) jona, proces bioluženja, parcijalni najmanji kvadrati, veštačka neuronska mreža.